Real-time Friction Estimation for Grip Force Control

Heba Khamis, *Member IEEE*, Benjamin Xia, and Stephen J. Redmond, *Senior Member, IEEE*

***Abstract*—An important capability of humans when performing dexterous precision gripping tasks is our ability to feel both the weight and slipperiness of an object in real-time, and adjust our grip force accordingly. In this paper, we present for the first time a fully-instrumented version of our PapillArray tactile sensor concept, which can sense grip force, object weight, and incipient slip and friction, all in real-time. We demonstrate the real-time estimation of friction and 3D force from PapillArray sensors mounted on each finger of a two-finger gripper, combined with a closed-loop grip-force control algorithm that dynamically applies a near-optimal grip force to avoid dropping objects of varying weight and friction. A vertical lifting task was performed using an object with varying weight and friction, and with some common household items. After intentionally adding a 20% safety margin on the target grip force, the actual grip force applied was only 9-30 % greater than that required to avoid slip. Future work will focus on incorporating real-time torque measurement into the grip force feedback control. This will significantly advance the state-of-the-art in artificial tactile sensing and bring us closer to robotic dexterity.**

I. Introduction

A. Humans quickly adjust their grip force for friction

The human hand can perform complex object manipulation with ease. Each of our fingertips contains ~2,000 mechanoreceptors embedded in the glabrous (hairless) skin regions, which individually sense vibration, pressure and skin-stretch [1], and as a population can provide information about object shape [2], texture, and even friction [3]; in fact, humans can estimate the friction of a surface and adjust the grip force accordingly within 100 ms of contacting an object during lifting experiments [4]. This friction-sensing ability is critical to our dexterity during precision gripping; i.e., using a two-fingered pincer grasp.

B. Tactile sensors that sense incipient slip and/or friction

However, the vast majority of tactile sensors lack any such friction-sensing capability. The majority of existing tactile sensors focus on determining (predominantly) normal forces and (occasionally) tangential forces at the contact interface [5]. While these quantities are important, they alone provide insufficient information to successfully perform precision (i.e., two-fingered) grasping and manipulation.

* Research supported by the Office of Naval Research (US Department of the Navy) / Navy and Marine Corps Science and Technology [GRANT12395989], Australian Research Council Future Fellowships [FT130100858], and Science Foundation Ireland President of Ireland Future Research Leaders Award [17/FRL/4832].

H. Khamis, B. Xia, and S. J. Redmond are with the Graduate School of Biomedical Engineering, UNSW Sydney, Sydney Australia (phone: +61293853911; e-mail: h.khamis@unsw.edu.au).

S. J. Redmond is also with the UCD School of Electrical and Electronic Engineering, the UCD Centre for Biomedical Engineering, and SFI Insight Centre for Data Analytics. University College Dublin, Dublin, Ireland.

The critical information which they do not measure relates to other properties (i.e., the coefficients of static (μ_s) and dynamic friction) and interactions (incipient/partial and overt/complete slip) at the interface between the gripper fingers and the object being manipulated. μ_s is a key parameter that influences the minimum grip (i.e., normal to the gripper fingers) force required to hold an object of a specific weight (generating forces tangential to the gripper fingers). In certain grip poses, if μ_s is accurately estimated and the tangential forces can also be measured, then the grip force can be adjusted to securely hold the object.

1) Estimating friction on initial contact or after overt slip

Older methods, which attempt to detect gross slip of an object and estimate μ_s during this gross slip event in order to adjust the grip force so as to arrest the slip [6-9], may be undesirable, as the gripper may respond too slowly to arrest the slip [10]. Some sensors attempt to detect μ_s on initial contact as the sensor splays outwards across the object with increasing normal force; however, these sensors have a limited range and/or poor precision [11], or are overly complex, thus present significant miniaturisation challenges [12]; these sensors are also unable to later update estimates of μ_s should the frictional conditions change over time [10].

2) Estimating friction from incipient slip

Another approach to achieving robotic grip security has been to detect incipient slip and then increase the grip force by some prescribed amount following such an event; incipient slip is defined as relative shear displacement on the sensing surface caused by slippage of part, but not all, of the contact interface. Various sensors are described in the literature for measuring incipient slip [10]. However, again, without knowing μ_s, it is unknown if the selected grip force adjustment will be sufficient to arrest the slip.

Fortunately, it is possible to estimate μ_s from incipient slip. This is a powerful approach because the object has not yet overtly slipped, and so knowledge of the friction and forces at the contact interface allows the grip force to be optimally adjusted to arrest the propagation of incipient slip across the contact and prevent an overt slip from occurring.

Tremblay *et al.* [13] used the difference in vibration magnitude measured by two accelerometers to detect incipient slip on the periphery of their tactile sensor, and at that time took the ratio of total tangential to total normal force experienced by the sensor to estimate μ_s. This method has two potential limitations: (i) detecting incipient slip using vibration is not robust against interfering environmental vibration (i.e., motors), and; (ii) this approach will underestimate μ_s because the average contact pressure over the contact area is larger than the local contact pressure at the location of slip. This will result in a larger than necessary grip force being applied. We will address both limitations in this paper, by using shear displacement to detect incipient slip, and by measuring forces at the location were slip occurs.

C. Innovation

Our group previously published a tactile sensing concept to estimate μ_s from incipient slip occurring on one or more silicone pillars in an array called the PapillArray [14]. In this proof-of-concept design: (i) discrete pillars allow different regions of the contact interface to move and slip independently, and; (ii) by using different height pillars, a non-uniform pressure and hence traction distribution across the sensor array is established when gripping an object, encouraging slip to occur first on the shorter pillars, where the normal force (and hence traction) is lowest. Then, by subsequently estimating the normal and tangential forces on a pillar which has just slip, μ_s could be estimated.

However, in [14], the sensor *was not instrumented*. The sensor constituted one homogenous piece of silicone, slip events were determined using an external video camera, and forces on each pillar were estimated indirectly by distributing global normal and tangential force (measured at the location where the sensor was mounted) onto each of nine silicone pillars according to a simple linear elastic model.

Later, further developing of this concept, we published a novel optical sensing technique to measure 3D displacements and 3D forces experienced by one *single* silicone pillar [15].

Now, in this paper, we further miniaturise the design presented in [14] and instrument each of the nine silicone pillars using the optical technique presented in [15]. Furthermore, we demonstrate the real-time operation of two PapillArray sensors in a range of simple lifting tasks, where the sensor outputs (real-time 3D force, incipient slip detection, and friction estimation) are used to dynamically set the target grip force for a two-finger gripper. We show that measuring friction in real-time allows the grip force to be optimized/minimized to avoid dropping the unknown objects.

We emphasise, never before has a sensor been able to detect incipient slip and accurately measure normal and tangential forces at the location of slip to estimate μ_s.

D. Scope

Due to the difficulty of the challenge of real-time detection of incipient slip and friction estimation, and subsequent real-time grip force control, we limit the scope of this work to gripping flat parallel-surfaced objects and lifting them vertically. Beyond the scope of this work are the even more challenging tasks of controlling the grip force when there is torque at the contact (when gripping off-centre), or when the surface is curved or compliant. These advancements will be the focus of future work.

II. Methods

A. PapillArray sensor

The design concept of the PapillArray sensor is described in [14]. The PapillArray sensor is an array of silicone pillars with different unloaded heights. When the sensor is pressed against a surface or object, the difference in pillar heights encourages each of the pillars to experience a different normal force (resulting in a different traction). When a tangential force is also applied, this distributes approximately uniformly across the pillars. This means that the ratio of tangential-to-normal force experienced by each pillar is different. As the tangential force increases, the first pillar whose tangential-to-normal force ratio exceeds μ_s will slip. As the tangential force increases further, the next pillar whose tangential-to-normal force ratio exceeds μ_s will slip next, and so on, until the last pillar slips (resulting in overt/gross slip of the object against the sensor). The new miniaturised PapillArray sensor is shown in Fig. 1A with the pillar dimensions Fig. 1B-D. Two identical PapillArray sensors were used in this work.

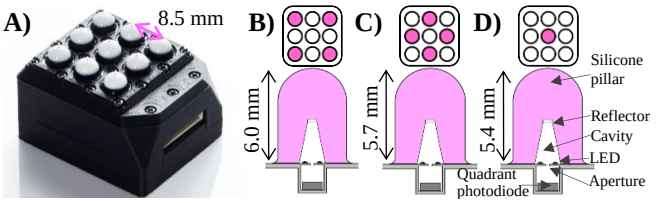

Figure 1. A) Photograph of a PapillArray sensor, and dimensions of the B) corner (shortest) pillars C) middle-height pillars, and D) central (tallest) pillar. For all pillars, the pillar outer diameter is 6 mm, the diameter of the base of the conical cavity is 4 mm, the reflector diameter is 2 mm, the aperture diameter is 0.8 mm, the reflector to aperture distance is 3.5 mm. and distance from the aperture to the top of quadrant photodiode is 2.0 mm.

The instrumentation of the PapillArray pillars is described in [15]. Briefly, for each pillar of the PapillArray sensor, a camera obscura is created by making a pinhole aperture on a printed circuit board at the base of the silicone pillar, and embedding a diffuse reflector disk at the top end of a hollow cavity that is moulded inside the silicone pillar (Fig. 1D). The diffuse reflector is illuminated by two light-emitting diodes on either side of the pinhole aperture. Below the aperture, the inverted image of the reflector disk is projected onto a quadrant photodiode (i.e., four photodiodes in a segmented configuration). The projected image of the disk appears as a spot of light; the shape, position, and area of the projected light spot depend primarily on the 3D orientation and XYZ displacement of the reflector disk. The four measurements of light incident on each of the four photodiode quadrants are used to infer 3D displacement and 3D force, using two independent calibration mappings.

Each of the eighteen pillars in the two PapillArray sensors was calibrated as described in [15]. Briefly, this involved applying pre-defined patterns of deflection to each pillar individually using an XYZ stage. Deflection of the pillars in 3D was verified using point tracking applied to a simultaneously-recorded video of the external pillar tips (and stage Z position), and 3D forces acting on the pillar were verified against the signals from a 3D force/torque sensor (Mini40, ATI Industrial Automation, USA). For each PapillArray sensor, two distinct multivariate polynomial regression models (2^{nd} order) were trained (using MATLAB R2018a, Mathworks, USA) using a training data set: (i) four photodiode outputs mapped to the three XYZ displacement coordinates, and; (ii) four photodiode outputs mapped to three orthogonal force vector components. The resulting polynomials were then validated on a testing data set.

B. Real-time slip detection and friction estimation

When the pillars of a PapillArray sensor are loaded with a tangential force, they are deflected away from their unloaded positions. While a pillar is stuck (not slipping) against an object and the tangential force increases, this shear deflection also increases at approximately the same rate as the object moves relative to the rigid part of the sensor. When a pillar slips, it stops deflecting at the same rate as the object moves,

and the other pillars which are yet to slip continue moving with the object relative to the sensor. Here, the slip detection procedure is initiated whenever the pillar under the greatest normal force (denoted as the reference pillar) experiences a tangential load (> 0.5 N tangential force). A pillar that is in contact (> 0.25 N normal force when the slip detection procedure begins) was detected to have slipped when the magnitude of its tangential velocity first drops (arbitrarily) below 60% of the tangential velocity of the reference pillar; this velocity threshold percentage will trade off slip detection robustness against slip detection latency. Slip detection ceases when the tangential velocity of the reference pillar drops to (arbitrarily) below 50% of its peak value during the slip detection phase; in this case, the reference pillar is either itself slipping, or the grip force correction has arrested the tangential deflection. In the case of two PapillArray sensors integrated into the gripper system, slip detection is performed for each sensor independently.

When a pillar was detected to have slipped, the ratio of tangential-to-normal force acting on that pillar at the moment of slip was taken as the current estimate of μ_s for that sensor; any previous estimates of μ_s from that sensor are discarded and replaced by this most recent estimate. In the case of two PapillArray sensors integrated into a gripper system, the μ_s is estimated for each sensor independently; i.e., there will be an estimate of μ_s from each of the two sensors relating to two sides of the object being grasped.

The two calibration mapping models (3D displacement and 3D force) and the incipient slip detection and friction estimation algorithms for the two PapillArray sensors were implemented in Java, running in real-time on a PC, with the signals from all eighteen four-quadrant photodiodes being streamed through a serial port at a 1000 Hz sampling rate.

C. Two-finger gripper

The two-finger gripper was a modified 2F-140 (Robotiq, Quebec, Canada). The motor of the gripper was replaced with a stepper motor (NEMA 17, 1.8° step angle). A PapillArray sensor was mounted on each finger of the gripper (Fig. 2).

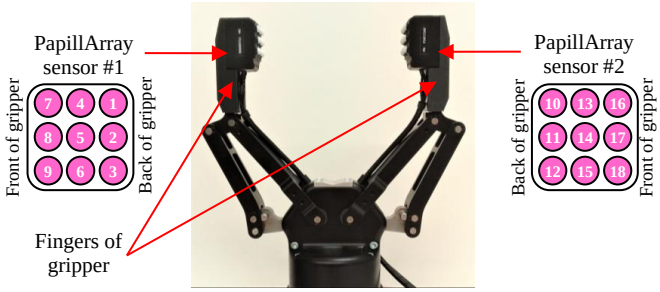

Figure 2. Modified Robotiq 2F-140 gripper two-finger gripper with a PapillArray sensor mounted on each finger. Pillar labels (1-18) also shown.

D. Grip-force controller

A microcontroller (Due; Arduino, Italy) streamed the digitized photodiode signals to a PC where the 3D deflection and 3D forces were resolved, incipient slip was detected, and the target grip force was calculated (described below) using the abovementioned Java application.

The total grip (normal) force magnitude applied by each PapillArray sensor was resolved by summing the normal (compressive) forces on each of the nine pillars of that sensor:

$$F_{N,1} = \sum_{i=1}^{9} F_{z,i} \text{ and } F_{N,2} = \sum_{i=10}^{18} F_{z,i}\,, \quad (1)$$

where $F_{N,1}$ is the total grip force applied by PapillArray sensor #1 (on the left finger of the gripper pictured in Fig. 2), $F_{N,2}$ is the total grip force applied by PapillArray sensor #2 (on the right finger of the gripper pictured in Fig. 2) and $F_{z,i}$ is the compressive force on pillar $i \in \{1,...,18\}$, where pillars 1-9 are on sensor #1 and pillars 10-18 are on the sensor #2.

The total load (tangential) force magnitude acting on each PapillArray sensor was resolved by summing the tangential forces on each pillar of that sensor:

$$|F_{T,1}| = \sqrt{\left(\sum_{i=1}^{9} F_{x,i}\right)^2 + \left(\sum_{i=1}^{9} F_{y,i}\right)^2} \quad (2)$$

$$|F_{T,2}| = \sqrt{\left(\sum_{i=10}^{18} F_{x,i}\right)^2 + \left(\sum_{i=10}^{18} F_{y,i}\right)^2} \quad (3)$$

where $|F_{T,1}|$ and $|F_{T,2}|$ are the magnitude of the tangential force acting on PapillArray sensor #1 and sensor #2, respectively, and $F_{x,i}$ and $F_{y,i}$ are the resolved tangential forces on pillar $i \in \{1,...,18\}$.

The grip force error was calculated as the difference between the target grip force (F_N; described in section II.*E.*) and the grip force from the sensor experiencing the lower of the two grip forces (note, we expect $F_{N,1} \approx F_{N,2}$):

$$e = F_N - \min(F_{N,1}, F_{N,2}). \quad (4)$$

This error (e) was sent from the PC to a second microcontroller which performed PID control to actuate the motor of the two-finger gripper in order to achieve the target grip force. A block diagram of the system is shown in Fig 3.

E. Experimental protocol

The gripper was mounted on a vertical linear stage (T8x4 lead screw, 300 mm stroke) actuated using a stepper motor (NEMA 17, 1.8° step angle) – see Fig. 4. After the gripper makes initial contact with the object to be lifted, the vertical stage moves the gripper upwards a total of 10 mm (the lifted position) with a velocity of 10 mm.s^{-1} and an acceleration of 50 mm.s^{-2}. The vertical stage remains at the lifted position for 5 s, and the relative movement between the object and the gripper are observed visually with the aid of markings on the object and a rigid pointer on the gripper. The lift is considered *successful* (✓) if the object has not slipped (object moved downwards less than 0.5 mm with respect to the gripper) during this time. If the object has slipped between 0.5 and 5 mm during this time, then the result is considered to be *very slow gross slip* (~). The lift is considered *unsuccessful* (×) if the object has slipped by more than 5 mm with respect to the gripper during this time.

A custom object with replaceable surfaces and adjustable weight was 3D printed from PLA thermoplastic using an Ultimaker 3 printer (Ultimaker B.V., Netherlands) – see Fig 4B. In total, there were four combinations of weight and surface material: two weights (light and heavy) and two surface materials (low friction – lubricated (Unilube; Griffon, Netherlands) paper; and high friction – cardboard). Each object was lifted five times for each grip-force control strategy investigated (one dynamic grip-force control strategy, and five fixed grip-force control strategies with different fixed target grip forces), which are described below.

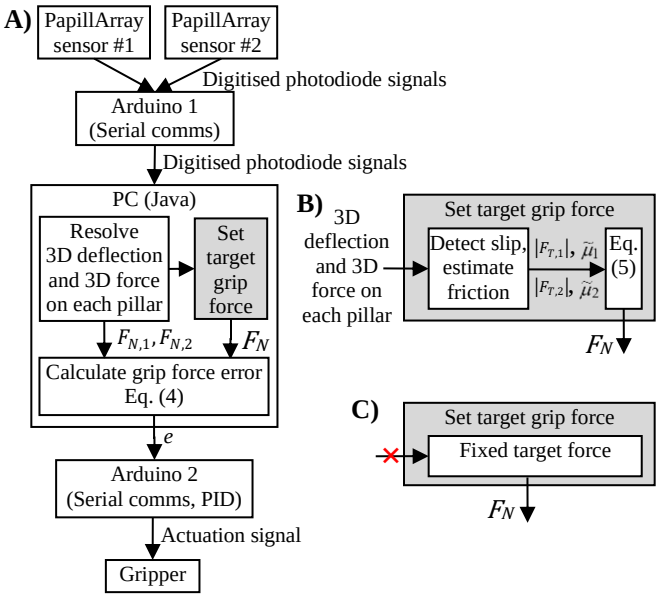

Figure 3. A) Block diagram of gripper system, setting the target grip force in the B) dynamic grip force control strategy, and C) fixed grip force control strategy which does not use any tangential force or friction information from the PapillArray sensor (only normal force from the PapillArray is used).

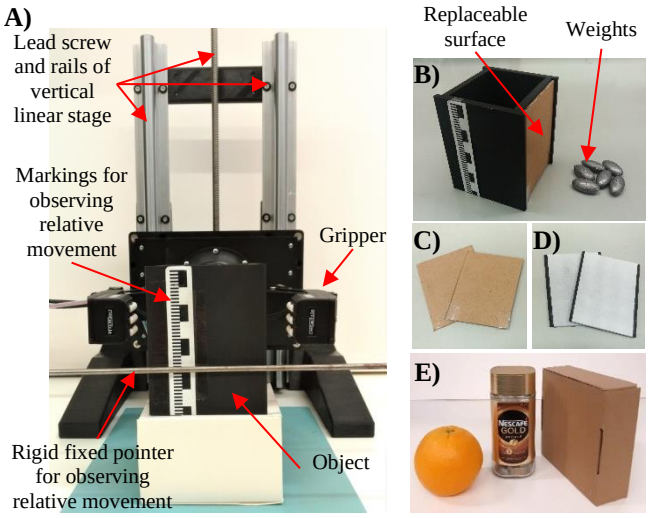

Figure 4. A) Photograph of experimental test rig. The gripper closes and achieves a target grip force on the object. The vertical linear stage then lifts the gripper up 10 mm. During the lifting phase, each PapillArray will detect slip of one or more of its nine pillars, and from the forces on these slipping pillars estimate the friction, which is subsequently used to set a target grip force that is sufficient to secure the grasp on the object. B) Photograph of the object with replaceable surfaces and adjustable weight, C) lubricated paper surface, D) cardboard surfaces, and E) household items.

1) Dynamic grip force control

For dynamic grip force control, the grasp is initiated with a target grip force of 4 N, such that at least two pillars from each PapillArray sensor make contact with the object. The robot arm then lifts the gripper. During the lifting phase, following the first pillar slip detection, the target grip force (F_N) is dynamically determined according to:

$$F_N = \max\left(4,\quad 1.2 \times \left|F_{T,1}\right|/\tilde{\mu}_1\,,\quad 1.2 \times \left|F_{T,2}\right|/\tilde{\mu}_2\,,\right), \qquad (5)$$

where a 20% safety margin is used, $\left|F_{T,1}\right|$ (Eq. (2)) and $\left|F_{T,2}\right|$ (Eq. (3)) are the magnitude of the tangential force acting on PapillArray sensor #1 and #2, respectively, $\tilde{\mu}_1$ and $\tilde{\mu}_2$ are the current estimates of friction from PapillArray sensors #1 and #2, respectively. A minimum target grip force of 4 N is maintained to prevent pillars from losing contact with the object.

2) Fixed grip force control

Five different fixed target grip force (F_N) values were tested: 4, 6, 9, 14, and 20 N – each fixed force is 50% larger (to the nearest whole number) than the previous fixed force. The test protocol here was the same as the dynamic grip force control protocol, except that the target grip force remained constant throughout the initial contact and lifting phases.

F. Household objects

Some common household items (Fig 4E) were also lifted using the dynamic grip force control. These were: an orange, a jar of coffee and a cardboard box. The final target grip force for the dynamic grip force control was compared to the minimum required grip force for a successful lift, which was determined by lifting using fixed grip force control at target grip forces from 4 N in 1 N increments until a successful lift.

III. Results

A. PapillArray pillar force and displacement accuracy

In Table I we show the pooled displacement and force estimation errors for all eighteen pillars of the two PapillArray sensors used in this work.

TABLE I. Displacement and Force Error Statistics Across All Eighteen Pillars of Two PapillArray Sensors. Full-Scale (FS).

Pillar axis	Displacement (mm)		Force (N)	
	FS	Error (mean ± SD)	FS	Error (mean ± SD)
X	±1.0	0.032 ± 0.035	±1.5	-0.001 ± 0.075
Y	±1.0	0.031 ± 0.043	±1.5	0.004 ± 0.059
Z	+1.5	0.050 ± 0.330	+6.0	0.072 ± 0.395

B. Lifting an object with varying weight and friction

Example outputs of the PapillArray sensor during the lifting task using dynamic grip-force control for the heavy custom-made object with a lubricated paper surface (low friction) are shown in Fig. 5, and lifting the lighter custom-made object with a cardboard surface (high friction) shown in Fig. 6. For both trials, the object was successfully lifted.

Different friction estimates were obtained for the two different object surfaces – for the heavy object with lubricated paper surface (Fig. 5C), the friction estimate for sensor #2 was updated three times: $\tilde{\mu}_2$= 0.38, 0.30 and 0.35 at 2.51 s, 2.52 s and 2.55 s due to slip detection on pillars 12, 17 and 11, respectively, and the friction estimate for sensor #1 was updated twice: $\tilde{\mu}_1$= 0.27 and 0.44 at 2.55 s and 2.56 s due to slip detection on pillars 6 and 2, respectively; for the light object with cardboard surface (Fig. 6C), the friction estimate for sensor #1 was updated twice: $\tilde{\mu}_1$= 0.83 and 0.43 at 2.58 s and 2.61 s due to pillars 2 and 3 slipping, respectively, and the friction estimate for sensor #2 was updated just once: $\tilde{\mu}_2$= 0.46 at 2.60 s due to slip detection on pillar 11. Different tangential forces were also measured for the different object weights – for the heavy object (788 g, ~7.73 N), the final tangential force magnitudes were $\left|F_{T,1}\right|$ =

4.03 N and $|F_{T,2}|$ = 3.83 N (Fig. 5A); and for the light object (431 g, ~4.23 N), the final tangential force magnitudes were $|F_{T,1}|$ = 2.24 N and $|F_{T,2}|$ = 2.10 N (Fig. 6A). The different friction estimate and tangential force measurements resulted in a different target grip force in each case – a final grip force of 15.00 N for the heavy object with lubricated paper surface, and 6.36 N for the light object with cardboard surface.

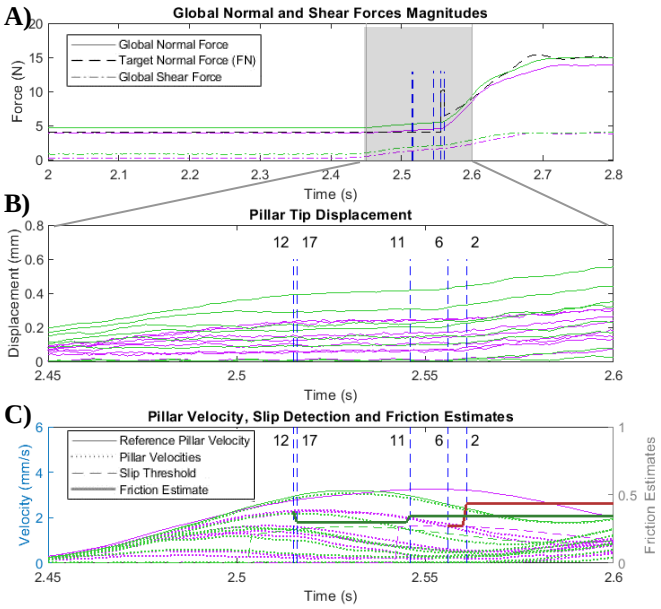

Figure 5. Example of sensor output during lifting task with dynamic grip-force control. Heavy custom-made object (788 g, ~7.73 N) with lubricated paper (low friction) surface: A) global shear and normal force magnitudes, B) tangential pillar displacements for shaded region in A), and C) tangential pillar velocities, slip detection and friction estimates for shaded region in A). Green lines for PapillArray sensor #1 and purple lines for PapillArray sensor #2. Vertical dashed lines indicate pillar slip detection (numbers indicate pillar label, as per Fig. 2).

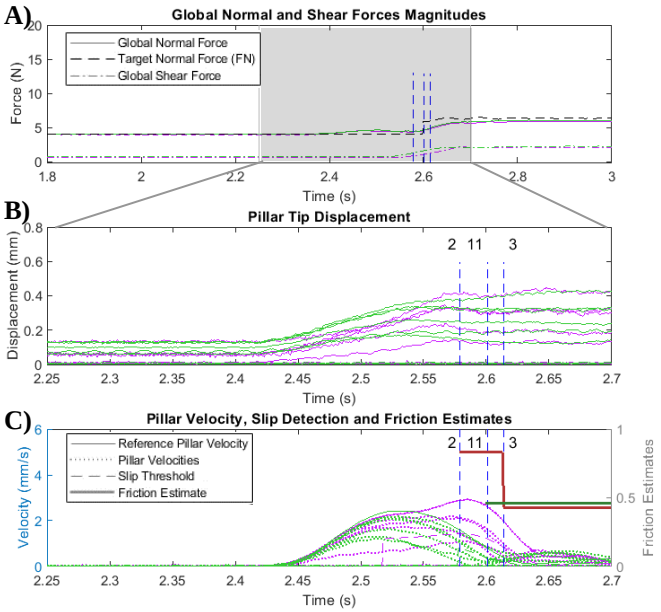

Figure 6. Example of sensor output during lifting task with dynamic grip-force control. Light custom-made object (431 g) with cardboard surface (high friction). See Fig. 5 caption for other information.

The results of 120 lifting trials for the custom object (2 weight conditions × 2 surface material combinations × 5 repetitions × (dynamic grip force + 5 × fixed grip force)) are shown in Table II. Using the friction and load-dependent dynamic grip force (determined using the PapillArray sensor outputs) always resulted in a successful lift, and the final (5 s after the end of the lifting phase) target grip force used during these trials was always near-optimal; the final target grip force is 11-30 % greater than the fixed grip force that resulted in a very slow slip and less than the smallest fixed grip force where lifting was successful, for the same weight and surface material.

Table III shows the results of lifting common household items using the dynamic grip force control. The final target grip force F_N was 9-30 % larger than the minimum grip force required for a successful lift (< 0.5 mm slip in 5 seconds), indicating that a near-optimal grip force is determined by the PapillArray sensors.

IV. Discussion

A. Summary of results

In this work, a closed-loop real-time friction- and load-dependent grip force control system has been described which uses the friction estimate and 3D resolved forces determined by two PapillArray sensors (one on each finger of the two-finger gripper). The system has been validated with a simple experiment in which an object with varying weight and friction (two weights, two different surface materials), and some household items, were grasped and lifted vertically using the sensor-determined dynamic grip force. The dynamic grip force was shown to be near-optimal (i.e., near minimal without invoking object slip) when compared to applying a predetermined fixed grip force.

B. Discussion of related work

Besides the PapillArray sensor, there are currently no resoundingly successful tactile sensors that can detect incipient slip *and also* measure friction without requiring gross slip to occur [10]. Perhaps the most successful of the incipient slip sensors is the GelSight/GelSlim sensor family [16, 17]. A transparent elastomer skin is patterned so the sensor's surface movements can be tracked using video. This allows the measurement of relative displacement of different regions of the contact area. These sensors can reliably detect incipient slip [18], but cannot estimate friction so as to suggest an appropriate grip force; in [18], the grip is simply increased in 10 N increments whenever incipient slip is detected. More recently, inverse finite element modelling has enabled force distribution estimates from gel displacements, which could facilitate friction estimation from incipient slip [19]. The gel and patterning used in these sensors have also shown limited long-term durability [17]. A similar sensor is described in [20], whereby a camera tracks the overlap and color mixing of colored markers in two layers of elastomer for measuring the distributed 3D motion of a surface, but these displacements have not yet been resolved to measure local force or subsequently estimate friction. More recently, similar camera-based designs have been presented, such as the Soft Bubble Gripper [21] and DIGIT [22]. In general, these camera-based systems have several inherent limitations related to the ability to sense normal force, low sampling rate

TABLE II. RESULTS OF LIFTING CUSTOM OBJECTS WITH DIFFERENT WEIGHTS AND SURFACE MATERIALS USING DYNAMIC GRIP FORCE CONTROL (SHOWING MEAN ± SD OF *FINAL* (5 S AFTER THE END OF THE LIFTING PHASE) FRICTION ESTIMATE, TANGENTIAL FORCE MAGNITUDE, AND NORMAL FORCE MAGNITUDE FOR EACH SENSOR, AND *FINAL* TARGET GRIP FORCE F_N) AND FIXED GRIP FORCE CONTROL.

Surface	Weight	Dynamic grip force			Fixed grip force				
		Sensor #1	Sensor #2	F_N (N)	4 N	6 N	9 N	14 N	20 N
Cardboard	Light (431 g) (~4.23 N)	$\tilde{\mu}_1$ = 0.59 ± 0.18 $\lvert F_{T,1} \rvert$ = 2.01 ± 0.05 N $F_{N,1}$ = 4.41 ± 1.30 N	$\tilde{\mu}_2$ = 0.54 ± 0.03 $\lvert F_{T,2} \rvert$ = 2.20 ± 0.04 N $F_{N,2}$ = 4.98 ± 0.28 N	✓✓✓ ✓✓ 5.21 ± 0.28	~~~ ~~	✓✓✓ ✓✓	✓✓✓ ✓✓	✓✓✓ ✓✓	✓✓✓ ✓✓
	Heavy (603 g) (~5.92 N)	$\tilde{\mu}_1$ = 0.65 ± 0.07 $\lvert F_{T,1} \rvert$ = 2.87 ± 0.02 N $F_{N,1}$ = 5.34 ± 0.71 N	$\tilde{\mu}_2$ = 0.50 ± 0.02 $\lvert F_{T,2} \rvert$ = 3.12 ± 0.01 N $F_{N,2}$ = 7.46 ± 0.28 N	✓✓✓ ✓✓ 7.46 ± 0.28	××× ××	~~~ ~~	✓✓✓ ✓✓	✓✓✓ ✓✓	✓✓✓ ✓✓
Lubricated paper	Light (510 g) (~5 N)	$\tilde{\mu}_1$ = 0.40 ± 0.01 $\lvert F_{T,1} \rvert$ = 2.37 ± 0.01 N $F_{N,1}$ = 7.20 ± 0.14 N	$\tilde{\mu}_2$ = 0.32 ± 0.00 $\lvert F_{T,2} \rvert$ = 2.84 ± 0.02 N $F_{N,2}$ = 10.51 ± 0.06 N	✓✓✓ ✓✓ 10.51 ± 0.06	××× ××	××× ××	~~~ ~~	✓✓✓ ✓✓	✓✓✓ ✓✓
	Heavy (788 g) (~7.73 N)	$\tilde{\mu}_1$ = 0.40 ± 0.07 $\lvert F_{T,1} \rvert$ = 3.90 ± 0.14 N $F_{N,1}$ = 12.12 ± 3.10 N	$\tilde{\mu}_2$ = 0.34 ± 0.00 $\lvert F_{T,2} \rvert$ = 4.25 ± 0.14 N $F_{N,2}$ = 14.93 ± 0.52 N	✓✓✓ ✓✓ 15.65 ± 1.14	××× ××	××× ××	××× ××	~~~ ~~	✓✓✓ ✓✓

✓ = successful lift (< 0.5 mm slip in 5 seconds); ~ = very slow gross slip (between 0.5 and 5 mm of slip in 5 seconds); and × = unsuccessful lift (> 5 mm slip in 5 seconds)

TABLE III. RESULTS OF LIFTING HOUSEHOLD ITEMS USING DYNAMIC GRIP FORCE CONTROL (SHOWING *FINAL* TARGET GRIP FORCE F_N (MEAN ± SD OF FIVE REPETITIONS)) AND MINIMUM FIXED GRIP FORCE FOR SUCCESSFUL GRIP.

Item	Weight (g)	F_N (N) (mean ±SD)	Succesful* min. grip force (N)
Orange	347	6.10 ± 0.60	5
Cardboard box	770	8.79 ± 0.58	8
Coffee jar	781	13.00 ± 0.81	10

* Successful lift: < 0.5 mm slip in 5 seconds.

(limited by camera frame rate), and the minimum size of the sensor (limited by camera focal length and/or depth of field); low frame rate is also expected to limit incipient slip detection accuracy for compliant objects due to an inability to sense associated vibrations associate with slip events.

A number of incipient slip sensors [16, 23-28] have been integrated into the fingers of robotic grippers to demonstrate their utility in grip stabilization; of particular note is a capacitance-based silicone pillar array for detecting incipient slip, which is very similar to the PapillArray design [29]. However, none of these sensors are capable of determining an optimal grip force when incipient slip is first detected, and must heuristically adjust the grip until slip is arrested. The risk in this approach is that the required grip force may not be found before the object has dropped. The fundamental advantage of a sensor (like the PapillArray) that can both detect incipient slip and subsequently estimate friction at the instant that incipient slip is detected is that the required grip force is immediately estimated and can be quickly applied.

C. Experimental limitations

A number of experimental limitations need to be detailed. The slow lift motion was selected (velocity of 10 mm.s^{-1} and acceleration of 50 mm.s^{-2}) due to potential communications latencies in the grip force control loop; with a faster gripper and control loop, faster lifting speeds could be attempted.

Reference friction measurements were not made in this work, so the accuracy of the friction estimates during lifting were not validated. However, the near-optimality of the resulting performance is clear from the results, with the gripper applying a minimal/optimised grip force (> largest fixed grip force resulting in a very slow gross slip, and < smallest fixed grip force where lifting was successful).

The object shape and compliance (which was a relatively flat, yet coated in a somewhat compliant surface) was kept the same throughout the experiment. Future experiments are planned which will validate the system with curved surfaces and compliant materials, where incipient slip detection and subsequent estimation of coefficient of friction will be made more challenging by the variable orientation between the object surface and the sensor frame of reference.

Another limitation of the experimental procedure here is that the lift motion was vertical only and grasp applied approximately near the centreline of the objects, and hence did not generate any significant torque loads on the contact interface between the PapillArray sensor and the objects lifted. Torques tangential to the fingertips are common during natural object manipulation, and most dexterous tasks are impossible without controlling for the effects of tangential torques [30]. Future work will attempt to modify the grip force control scheme presented here to handle both load forces *and torques* caused by gripping the object in such a way that the lifting force and weight force are not colinear.

D. Conclusions and future work

In this work, the utility of the PapillArray sensor concept [14, 15] as a real-time 3D force, incipient slip detection and friction estimation sensor has been demonstrated quantitatively in a series of simple vertical lifting tasks using objects with varying weights and surface materials; the dynamic friction- and load-dependent grip-force control achieved using the PapillArray sensor signals was shown to apply a near-optimal grip force irrespective of the weight and friction of the object, in contrast to an alternate approach of applying a fixed, pre-determined grip force. This is a behaviour of human manipulation never before artificially replicated. Future work will focus on incorporating real-time torque measurement into the grip force feedback control so objects can be grasped off-center or rotated. The challenges of detecting incipient slip and estimating friction for objects with curved or compliant surfaces will also be tackled. This will significantly advance the state-of-the-art in artificial tactile sensing and bring us closer to robotic dexterity.

REFERENCES

[1] Å. B. Vallbo and R. Johansson, "Properties of cutaneous mechanoreceptors in the human hand related to touch sensation," *Human Neurobiology*, vol. 3, no. 1, pp. 3-14, 1984.

[2] P. Jenmalm, I. Birznieks, A. W. Goodwin, and R. S. Johansson, "Influence of object shape on responses of human tactile afferents under conditions characteristic of manipulation," *European Journal of Neuroscience*, vol. 18, no. 1, pp. 164-176, 2003.

[3] H. Khamis, S. J. Redmond, V. Macefield, and I. Birznieks, "Classification of texture and frictional condition at initial contact by tactile afferent responses," in *International Conference on Human Haptic Sensing and Touch Enabled Computer Applications*, 2014: Springer, pp. 460-468.

[4] R. S. Johansson and G. Westling, "Roles of glabrous skin receptors and sensorimotor memory in automatic control of precision grip when lifting rougher or more slippery objects," (in English), *Experimental Brain Research*, vol. 56, no. 3, pp. 550-564, 1984/10/01 1984, doi: 10.1007/BF00237997.

[5] M. I. Tiwana, S. J. Redmond, and N. H. Lovell, "A review of tactile sensing technologies with applications in biomedical engineering," *Sensors and Actuators A: Physical*, vol. 179, pp. 17-31, 2012, doi: http://dx.doi.org/10.1016/j.sna.2012.02.051.

[6] R. Fernandez, I. Payo, A. S. Vazquez, and J. Becedas, "Micro-vibration-based slip detection in tactile force sensors," *Sensors*, vol. 14, no. 1, pp. 709-730, 2014.

[7] B. Choi, H. R. Choi, and S. Kang, "Development of tactile sensor for detecting contact force and slip," in *IEEE/RSJ International Conference on Intelligent Robots and Systems*, 2005: IEEE, pp. 2638-2643.

[8] Z. Su *et al.*, "Force estimation and slip detection/classification for grip control using a biomimetic tactile sensor," in *Proceedings of IEEE-RAS 15th International Conference on Humanoid Robots (Humanoids)*, 2015: IEEE, pp. 297-303.

[9] T. Okatani and I. Shimoyama, "A tactile sensor for simultaneous measurements of 6-axis force/torque and the coefficient of static friction," *Sensors and Actuators A: Physical*, vol. 315, p. 112362, 2020, doi: https://doi.org/10.1016/j.sna.2020.112362.

[10] W. Chen, H. Khamis, I. Birznieks, N. F. Lepora, and S. J. Redmond, "Tactile Sensors for Friction Estimation and Incipient Slip Detection – Towards Dexterous Robotic Manipulation: A Review," *IEEE Sensors Journal*, pp. 1-1, 2018, doi: 10.1109/JSEN.2018.2868340.

[11] T. Maeno, T. Kawamura, and S.-C. Cheng, "Friction estimation by pressing an elastic finger-shaped sensor against a surface," *IEEE Transactions on Robotics and Automation*, vol. 20, no. 2, pp. 222-228, 2004.

[12] K. Nakamura and H. Shinoda, "Tactile sensing device instantaneously evaluating friction coefficients," in *Technical Digest of the Sensor Symposium*, 2001, vol. 18, pp. 151-154.

[13] M. R. Tremblay and M. R. Cutkosky, "Estimating friction using incipient slip sensing during a manipulation task," in *Proceedings of IEEE International Conference on Robotics and Automation*, 2-6 May 1993 1993, vol. 1, pp. 429-434, doi: 10.1109/ROBOT.1993.292018.

[14] H. Khamis, R. I. Albero, M. Salerno, A. S. Idil, A. Loizou, and S. J. Redmond, "PapillArray: An incipient slip sensor for dexterous robotic or prosthetic manipulation–Design and prototype validation," *Sensors and Actuators A: Physical*, vol. 270, pp. 195-204, 2018.

[15] H. Khamis, B. Xia, and S. J. Redmond, "A novel optical 3D force and displacement sensor–Towards instrumenting the PapillArray tactile sensor," *Sensors and Actuators A: Physical*, vol. 291, pp. 174-187, 2019.

[16] W. Yuan, R. Li, M. A. Srinivasan, and E. H. Adelson, "Measurement of shear and slip with a GelSight tactile sensor," in *Proceedings of IEEE International Conference on Robotics and Automation*, 26-30 May 2015 2015, pp. 304-311, doi: 10.1109/ICRA.2015.7139016.

[17] E. Donlon, S. Dong, M. Liu, J. Li, E. Adelson, and A. Rodriguez, "GelSlim: A High-Resolution, Compact, Robust, and Calibrated Tactile-sensing Finger," in *2018 IEEE/RSJ International Conference on Intelligent Robots and Systems (IROS)*, 2018: IEEE, pp. 1927-1934.

[18] S. Dong, D. Ma, E. Donlon, and A. Rodriguez, "Maintaining Grasps within Slipping Bounds by Monitoring Incipient Slip," in *2019 International Conference on Robotics and Automation (ICRA)*, 2019: IEEE, pp. 3818-3824.

[19] D. Ma, E. Donlon, S. Dong, and A. Rodriguez, "Dense Tactile Force Estimation using GelSlim and inverse FEM," in *2019 International Conference on Robotics and Automation (ICRA)*, 2019: IEEE, pp. 5418-5424.

[20] X. Lin and M. Wiertlewski, "Sensing the Frictional State of a Robotic Skin via Subtractive Color Mixing," *IEEE Robotics and Automation Letters*, vol. 4, no. 3, pp. 2386-2392, 2019.

[21] N. Kuppuswamy, A. Castro, C. Phillips-Grafflin, A. Alspach, and R. Tedrake, "Fast Model-Based Contact Patch and Pose Estimation for Highly Deformable Dense-Geometry Tactile Sensors," *IEEE Robotics and Automation Letters*, vol. 5, no. 2, pp. 1811-1818, 2020, doi: 10.1109/LRA.2019.2961050.

[22] M. Lambeta *et al.*, "DIGIT: A Novel Design for a Low-Cost Compact High-Resolution Tactile Sensor With Application to In-Hand Manipulation," *IEEE Robotics and Automation Letters*, vol. 5, no. 3, pp. 3838-3845, 2020.

[23] T. Maeno, S. Hiromitsu, and T. Kawai, "Control of grasping force by detecting stick/slip distribution at the curved surface of an elastic finger," in *Proceedings of IEEE International Conference on Robotics and Automation*, 2000 2000, vol. 4, pp. 3895-3900, doi: 10.1109/ROBOT.2000.845338.

[24] J. Ueda, A. Ikeda, and T. Ogasawara, "Grip-force control of an elastic object by vision-based slip-margin feedback during the incipient slip," *IEEE Transactions on Robotics*, vol. 21, no. 6, pp. 1139-1147, 2005, doi: 10.1109/TRO.2005.853496.

[25] N. Watanabe and G. Obinata, "Grip force control based on the degree of slippage using optical tactile sensor," in *Proceedings of International Symposium on Micro-NanoMechatronics and Human Science*, 11-14 Nov. 2007 2007, pp. 466-471, doi: 10.1109/MHS.2007.4420900.

[26] S. Shirafuji and K. Hosoda, "Detection and prevention of slip using sensors with different properties embedded in elastic artificial skin on the basis of previous experience," *Robotics and Autonomous Systems*, vol. 62, no. 1, pp. 46-52, 2014, doi: http://dx.doi.org/10.1016/j.robot.2012.07.016.

[27] S. Dong, W. Yuan, and E. H. Adelson, "Improved gelsight tactile sensor for measuring geometry and slip," in *2017 IEEE/RSJ International Conference on Intelligent Robots and Systems (IROS)*, 2017: IEEE, pp. 137-144.

[28] J. W. James, S. J. Redmond, and N. F. Lepora, "A Biomimetic Tactile Fingerprint Induces Incipient Slip," *arXiv preprint arXiv:2008.06904*, 2020.

[29] T. M. Huh, H. Choi, S. Willcox, S. Moon, and M. R. Cutkosky, "Dynamically Reconfigurable Tactile Sensor for Robotic Manipulation," *IEEE Robotics and Automation Letters*, vol. 5, no. 2, pp. 2562-2569, 2020, doi: 10.1109/LRA.2020.2972881.

[30] I. Birznieks, H. E. Wheat, S. J. Redmond, L. M. Salo, N. H. Lovell, and A. W. Goodwin, "Encoding of tangential torque in responses of tactile afferent fibres innervating the fingerpad of the monkey," *The Journal of Physiology*, vol. 588, no. 7, pp. 1057-1072, 2010.

[31] H. Kinoshita, L. Bäckström, J. R. Flanagan, and R. S. Johansson, "Tangential torque effects on the control of grip forces when holding objects with a precision grip," *Journal of Neurophysiology*, vol. 78, no. 3, pp. 1619-1630, 1997.